Aerosol and Air Quality Research, 15: 2200–2211, 2015

ISSN: 1680-8584 print / 2071-1409 online
doi: 10.4209/aaqr.2015.04.0257

Chemical Composition and Light Extinction Contribution of $PM_{2.5}$ in Urban Beijing for a 1-Year Period

Huanbo Wang[1], Mi Tian[1], Xinghua Li[2*], Qing Chang[2], Junji Cao[3], Fumo Yang[1†], Yongliang Ma[4], Kebin He[4]

[1] *Key Laboratory of Reservoir Aquatic Environment of CAS, Chongqing Institute of Green and Intelligent Technology, Chinese Academy of Sciences, Chongqing 400714, China*
[2] *School of Chemistry and Environment, Beihang University, Beijing 100191, China*
[3] *Key Lab of Aerosol Chemistry & Physics, Institute of Earth Environment, Chinese Academy of Sciences, Xi'an 710075, China*
[4] *State Environmental Protection Key Laboratory of Sources and Control of Air Pollution Complex, School of Environment, Tsinghua University, Beijing 100084, China*

ABSTRACT

Daily $PM_{2.5}$ samples were collected in Beijing across four consecutive seasons from June 2012 to April 2013. Major water-soluble inorganic ions, carbonaceous species and elements were analyzed to investigate their temporal variations and evaluate their contributions to visibility impairment over different seasons and under different pollution levels. The mass concentrations of $PM_{2.5}$ ranged from 4.3 to 592.4 μg m^{-3}, with an annual average of 112.4 ± 94.4 μg m^{-3}. The predominant components of $PM_{2.5}$ were secondary inorganic ions (NH_4^+, NO_3^- and SO_4^{2-}) and carbonaceous compounds, which accounted for 45.9% and 24.1% of the total $PM_{2.5}$ mass, respectively. Distinct seasonal variation was observed in the mass concentrations and chemical components of $PM_{2.5}$. The average mass concentrations of $PM_{2.5}$ were the highest in winter, followed by spring, and lowest in autumn. Light extinction coefficients (b_{ext}) were discussed over four seasons. $(NH_4)_2SO_4$ was the largest contributor (28.8%) to b_{ext}, followed by NH_4NO_3 (24.4%), organic matter (19.5%), elemental carbon (7.4%), and coarse mass (7.2%), while fine soil, sea salt, NO_2 and Rayleigh made minor contributions, together accounting for 12.7% of b_{ext}. During the polluted periods, the contributions of $(NH_4)_2SO_4$ and NH_4NO_3 to b_{ext} increased dramatically. Therefore, in addition to control primary particulate emissions, the reduction of their precursors like SO_2, NO_x and NH_3 could effectively improve air quality and visibility in Beijing.

Keywords: Chemical composition; Reconstructed light extinction coefficient; Visibility; $PM_{2.5}$.

INTRODUCTION

$PM_{2.5}$ in the atmosphere have been found to be responsible for adverse health effects (de Kok *et al*., 2006; Pope and Dockery, 2006), climate change (Haywood and Boucher, 2000; Tai *et al*., 2010; Mahowald, 2011) and visibility degradation (Watson, 2002; Chang *et al*., 2009). The decline of visibility, particularly frequent hazes in megacities like Guangzhou, Chengdu and Beijing during the recent years (Tan *et al*., 2009; Zhao *et al*., 2011; Wang *et al*., 2013a), has become a major concern for the general public in China.

Visibility degradation is attributed to light absorption and light scattering by both gases and fine particle pollutants (Chan *et al*., 1999; Watson, 2002). However, fine particles are mostly responsible for the poor visibility, while the light extinction due to gas pollutants usually has a minor influence on urban visibility (Watson, 2002). A few measurements of surface aerosol optical properties have been conducted in polluted cities such as Beijing and Guangzhou (Garland *et al*., 2009; Jung *et al*., 2009; Fan *et al*., 2010). But it is difficult to determine the extinction properties of individual real particles due to their complex shapes and mixtures. At this time, light extinction coefficient (b_{ext}) could, instead, be reconstructed based on the chemical compositions of particles (Pitchford *et al*., 2007). An empirical formula relating b_{ext} to the chemical species of particles was established by the Interagency Monitoring of Protected Visual Environments (IMPROVE) network.

* Corresponding author.
Tel.: +86-10-82316160; Fax: +86-10-82314215
E-mail address: lixinghua@buaa.edu.cn
† Corresponding author.
Tel.: +86-23-65935921; Fax: +86-23-65935924
E-mail address: fmyang@cigit.ac.cn

Reconstruction of b_{ext} assumes that the particles are externally mixed and the mass extinction efficiency for each species is constant. Although these assumptions were not always satisfied, the reconstruction of b_{ext} is still a commonly used approach to identify key factors affecting the b_{ext} and ambient visibility (Cao *et al*., 2012; Zhang *et al*., 2012; Li *et al*., 2013a; Tao *et al*., 2014). Most recent studies have focused on analyzing mass concentrations, different chemical compositions, and sources of fine particles (He *et al*., 2001; Yao *et al*., 2002; Yang *et al*., 2011a; Yu *et al*., 2013). In addition, the studies in Beijing were mainly conducted during the important events, such as the 2006 Campaign of Air Quality Research and the 2008 Olympics (Li *et al*., 2012; Li *et al*., 2013a), or heavy pollution episode during wintertime in 2011–2013, especially in January 2013 (Wang *et al*., 2013b; Zhao *et al*., 2013a; Ji *et al*., 2014; Quan *et al*., 2014; Sun *et al*., 2014; Wang *et al*., 2014), all of which were short-term sampling and analysis. Recently, the seasonal characteristics of the chemical composition of $PM_{2.5}$ in Beijing have been determined during the 2009–2010 periods (Li *et al*., 2013b; Zhao *et al*., 2013b; Liu *et al*., 2014), whereas few of these previous studies have reported the contributions of each species to b_{ext}. An exception is that reported by Cao *et al*. (2012) for Xi'an. Furthermore, there is no study on reconstructing extinction coefficients based on the chemical compositions of $PM_{2.5}$ over four consecutive seasons in Beijing (Jung *et al*., 2009; Li *et al*., 2013a; Tian *et al*., 2014), especially on appointing the contribution of $PM_{2.5}$ chemical species to visibility degradation under different pollution levels and over different seasons.

In the present study, water-soluble inorganic ions, trace elements, organic carbon (OC) and elemental carbon (EC) during four different seasons were analyzed, and then seasonal variations of major components were investigated. Moreover, the apportionment of the chemical compositions of $PM_{2.5}$ for extinction effects was identified during different pollution levels. Understanding the impact of chemical compositions of $PM_{2.5}$ on b_{ext} will be very useful for the government agencies in their attempts to improve visibility and human health in Beijing.

METHODS

Site and Sampling

Sampling was conducted from 15 to 30 June and 10 to 20 August (representative of summer), 15 September to 21 October (autumn) in 2012, 5 January to 5 February (winter), and 4 March to 2 April (Spring) in 2013 at the campus of Beihang University (referred to as BHU, 39°59'N, 116°21'E) in urban Beijing. This sampling site is surrounded by the educational and residential districts without major industrial source. In addition, the sampling site is about 3.0 km southeast from Peking University and 2.8 km west from the Tower Division of the Institute of Atmospheric physics, which represent the general urban pollution in Beijing (Zhang *et al*., 2013; Tian *et al*., 2014).

Daily 23-h integrated $PM_{2.5}$ samples were collected using a five-channel Spiral Ambient Speciation Sampler (SASS, MetOne Inc.) with a flow rate of 6.7 L min^{-1}. The first channel was used to collect $PM_{2.5}$ with a 47 mm Teflon filter for $PM_{2.5}$ mass and elemental analysis. The second channel collected the particles for the analysis of water-soluble inorganic ions with a 47 mm Teflon filter. An MgO honeycomb denuder was set in front of the Teflon filter to reduce the acid gaseous interference. The third channel was used to collect $PM_{2.5}$ on quartz fiber filters for OC and EC analyses. The fresh quartz filters were pre-heated at 450°C in a muffle furnace for 4 h to remove any volatile components before sampling. The filter samples were stored in a freezer at –18°C before chemical analysis to minimize the evaporation of volatile components.

Meteorological data including wind speed (WS), temperature, relative humidity (RH) and precipitation were obtained from China Meteorological Data Sharing Service System (http://cdc.cma.gov.cn/home.do).

Gravimetric and Chemical Analysis

Before and after each sampling, the Teflon filters were conditioned at 22°C ± 5°C in relative humidity of 40% ± 5% for 24 h and then weighed using an electronic balance with a detection limit of 1 μg (Sartorius, Göttingen, Germany). Differences among replicate weights were less than 5 μg for each sample, which represented less than ± 5% of the total aerosol mass of the field samples.

Teflon filter from the second channel was extracted twice in 7.5 ml Milli-Q water via an ultrasonic bath for 20 min. The extracted water-soluble ions were filtered through a 0.45 μm PTFE syringe filter and stored at 4°C until analysis. Four anions (SO_4^{2-}, NO_3^-, Cl^-, and F^-) and five cations (Na^+, NH_4^+, K^+, Mg^{2+}, and Ca^{2+}) were determined by Ion chromatography ICS-1000 (Dionex Corp, Sunnyvale, CA.) with 2.4 mmol L^{-1} Na_2CO_3 and 0.3 mmol L^{-1} $NaHCO_3$ as the eluent and Ion chromatography ICS-2000 (Dionex Corp, Sunnyvale, CA.) with 20 mmol L^{-1} methanesulfonic acid (MSA) eluent, respectively. Field blank values were subtracted from sample concentrations.

A 0.5 cm^2 punch from each quartz filter was analyzed for OC and EC using a DRI Model 2001 Thermal/Optical Carbon Analyzer (Atmoslytic Inc., Calabasas, USA) following the IMPROVE thermal optical reflectance (TOR) protocol (Chow *et al*., 2007).

Specific elements from sodium to uranium were analyzed by Energy Dispersive X-ray fluorescence spectrometry (Epsilon 5 ED-XRF, PAN'alytical company, Netherlands) on Teflon filters. Quality assurance/Quality Control (QA/QC) procedures of the XRF analysis procedure were described by Xu *et al*. (2012a).

Data Analysis

The mass of $PM_{2.5}$ was reconstructed according to the method adopted by Zhang *et al*. (2013) and the revised IMPROVE method (Pitchford *et al*., 2007). $PM_{2.5}$ species were classified into eight major components: $(NH_4)_2SO_4$, NH_4NO_3, OM, EC, fine soil, sea salt, trace element oxide (TEO), and biomass burning-derived K.

The $(NH_4)_2SO_4$ mass was estimated by the SO_4^{2-} mass multiplied by a factor of 1.38, and the NH_4NO_3 mass was estimated by the NO_3^- mass multiplied by a factor of 1.29. OM was derived from multiplying OC concentrations by a

factor of 1.6 to account for unmeasured atoms, such as hydrogen, oxygen, and nitrogen in organic materials. The factor of 1.6 was employed in this study according to Xing *et al*. (2013), which demonstrated that the calculated OM/OC mass ratio in summer was relatively high (1.75 ± 0.13) and in winter was lower (1.59 ± 0.18) in $PM_{2.5}$ collected from 14 Chinese cities.

Sea salt was usually calculated by the Cl^- mass multiplied by a factor of 1.80 or by the Na^+ mass multiplied by a factor of 2.54. It should be noticed that most Cl^- may be contributed by coal combustion rather than sea spray in Beijing, especially during the heating period in winter and spring. Thus, we calculated sea salt using Na^+ by a factor of 2.54.

TEO was estimated following Zhang *et al*. (2013). The fine soil component was often estimated by assuming the elements mainly associated with soil be in their oxidized state (Al_2O_3, SiO_2, CaO, K_2O, FeO, Fe_2O_3 and TiO_2), which was thus calculated as follows:

$$[\text{Fine Soil}] = 2.20[\text{Al}] + 2.49[\text{Si}] + 1.63[\text{Ca}] + 2.42[\text{Fe}] + 1.94[\text{Ti}] \quad (1)$$

The total b_{ext} include the contributions of light scattering by particles (b_{sp}) and gases (b_{sg}), and light absorption by particles (b_{ap}) and gases (b_{ag}), where:

$$b_{ext} = b_{sp} + b_{ap} + b_{ag} + b_{sg} \quad (2)$$

The b_{ext} can be calculated based on revised IMPROVE algorithm:

$$\begin{aligned} b_{ext} \approx\ & 2.2 \times f_s(RH) \times [Small(NH_4)_2SO_4] \\ & + 4.8 f_L(RH) \times [Large(NH_4)_2SO_4] \\ & + 2.4 \times f_s(RH) \times [Small\ NH_4\ NO_3] \\ & + 5.1 f_L(RH) \times [Large\ NH_4\ NO_3] \\ & + 2.8 \times [Small\ OM] + 6.1 \times [Large\ OM] + 10 \times [EC] \\ & + 1 \times [Fine\ Soil] + 1.7 \times f_{ss}(RH) \times [Sea\ Salt] \\ & + 0.6 \times [PM_{2.5-10}] + 0.33 \times [NO_2(ppb)] \\ & + Rayleigh\ Scattering \end{aligned} \quad (3)$$

The apportionment of the total concentrations of $(NH_4)_2SO_4$ into the concentrations of the small and large size fraction in $PM_{2.5}$ was calculated according to Pitchford *et al*. (2007). The water growth adjustment term $f_s(RH)$, $f_L(RH)$ for small and large size distribution $(NH_4)_2SO_4$ and NH_4NO_3, and $f_{ss}(RH)$ for sea salt are used according to the water growth curves provided by Pitchford *et al*. (2007). The coarse mass was calculated by subtracting the $PM_{2.5}$ mass from the PM_{10} mass. The b_{ext} is in Mm^{-1}, chemical composition concentrations are in μg m^{-3}, dry efficiency terms are in unit of m^2 g^{-1}, and f (RH) is dimensionless.

RESULTS AND DISCUSSION

Temporal Variations of $PM_{2.5}$ Mass Concentration

The time series of daily $PM_{2.5}$ mass concentration in Beijing are illustrated in Fig. 1. Daily $PM_{2.5}$ concentrations ranged from 4.3 to 592.4 μg m^{-3} with an annual average of 112.4 ± 94.4 μg m^{-3} during the study period. The annual average was however lower than the 135 ± 63 μg m^{-3} measured on the Peking University campus in 2009 (Zhang *et al*., 2013), whereas it was comparable with the value observed in the TsingHua University campus during 2005–2006 (Yang *et al*., 2011a).

As illustrated in Fig. 1, daily $PM_{2.5}$ mass concentrations varied significantly during all four seasons. The $PM_{2.5}$ mass concentration, during the most polluted period (592.4 μg m^{-3}), was almost 150 times higher than that during the cleanest period (4.3 μg m^{-3}). There were seven heavily polluted periods with mass concentration of $PM_{2.5}$ exceeded 200 μg m^{-3}. What is worse, five severely polluted days, exceeding 300 μg m^{-3}, were observed in January of 2013. As shown in Fig. 2, during the pollution episodes in summer, autumn and winter, air masses were mainly from the south or southeast of Beijing, indicating that regional transport was important for the high level of $PM_{2.5}$ in Beijing. The mechanism for the formation of the severe haze episode in January 2013 was discussed by Wang *et al*. (2014), who showed that it was related to both the external factor of unfavorable meteorological conditions and the internal factors including rapid secondary transformation of primary gaseous pollutants to secondary aerosols.

The seasonal variations of $PM_{2.5}$ were evident. The average mass concentration of $PM_{2.5}$ was highest in winter, decreased in spring and summer, and was lowest in autumn. Daily $PM_{2.5}$ concentration exceeded the China National Ambient Air Quality Standards (75 μg m^{-3}) on 56.6% of days during all study periods, whereas it was 66.6% in summer, 24.2% in autumn, 75% in winter and 63.3% in spring, indicating that pollution in Beijing were serious and control measures should be undertaken to alleviate the $PM_{2.5}$ loading. Influenced by the increased emissions from residential heating and biomass burning, as well as the adverse dispersion and deposition conditions such as low wind speed and rare precipitation (Xu *et al*., 2012b), the mass concentration of $PM_{2.5}$ in winter was higher than any other seasons. The second highest seasonal $PM_{2.5}$ was observed in spring. The local crustal materials re-suspended into the atmosphere due to the stronger winds in spring might increase the $PM_{2.5}$ concentration (Zhang *et al*., 2012). The mass concentrations of $PM_{2.5}$ in summer were higher than the value in autumn, which were contradictory to the trends reported in the literature (Wang *et al*., 2011; Zhou *et al*., 2012; Zhao *et al*., 2013c). This may be explained by two reasons. One is that part of the sampling days in summer were in poor condition while the days of autumn were in good conditions. As shown in Fig. 1, the wind speeds were lower and the relative humidity was higher in summer than autumn, which is favorable for the accumulation of pollutants and the formation of second aerosols. Another one maybe the differences of photochemical reactions during the two seasons. Furthermore, it should be noticed that summer had more precipitation than any other seasons, yet not the lowest $PM_{2.5}$ level. This was likely because more secondary aerosols formed due to the high temperatures, and photochemical reactions may overwhelm the precipitation scavenging effect.

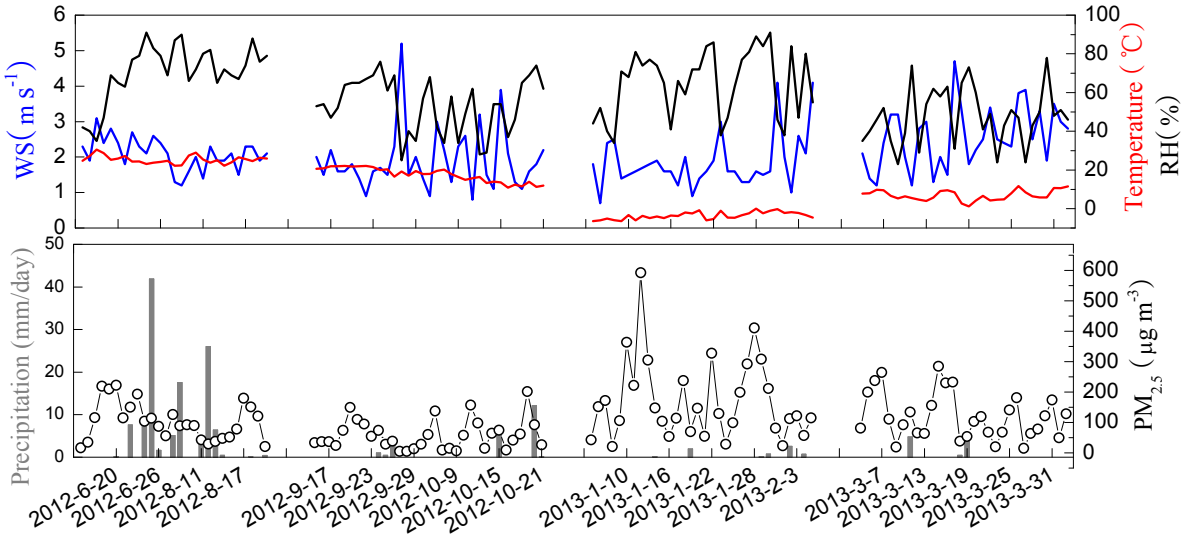

Fig. 1. Time series of measured $PM_{2.5}$ mass concentrations and meteorological parameters.

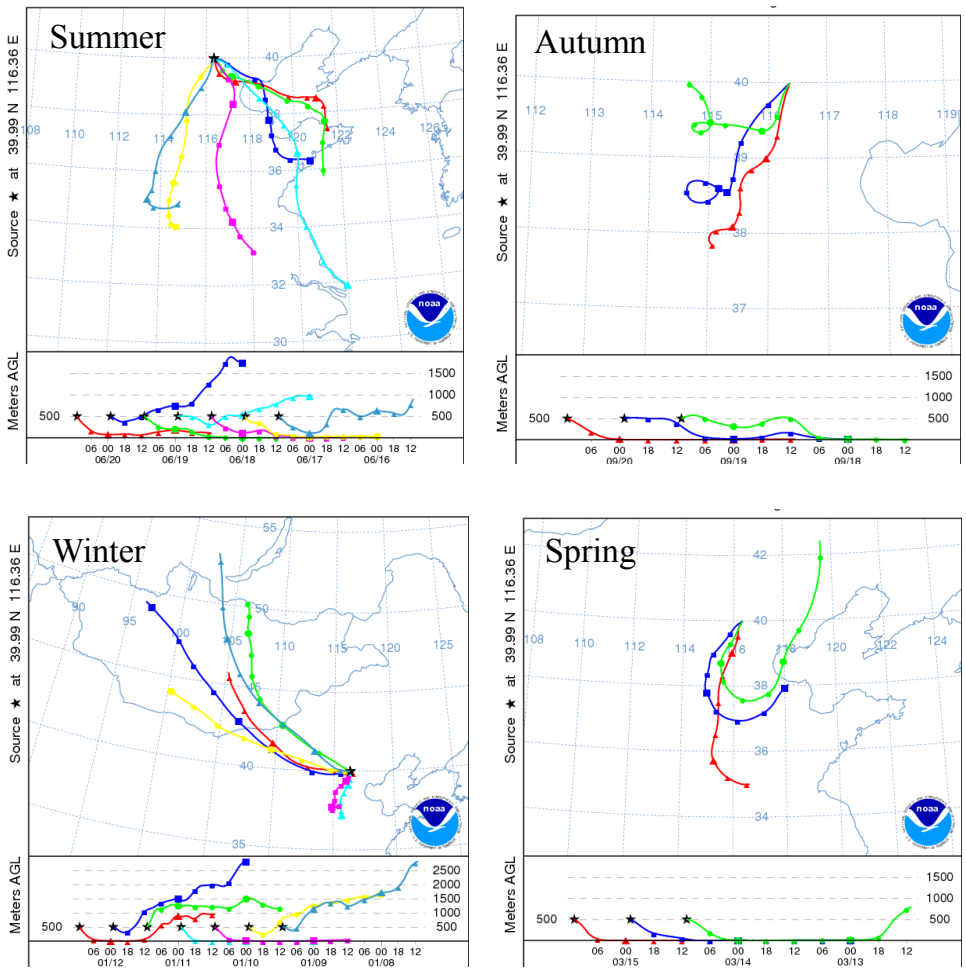

Fig. 2. 48-h back trajectories of air mass arriving in Beijing for typical pollution episode in different seasons.

Annual Average and Seasonal Variations of Water-Soluble Inorganic Ions

The daily mass concentrations of water-soluble inorganic ions (WSIIs) in $PM_{2.5}$ are illustrated in Fig. 3, and the average concentrations of each ion together with annual average values are listed in Table 1. The average concentration of the nine detected ions was 69.0 ± 61.8 μg m^{-3}, accounting for 57.8% of $PM_{2.5}$ mass concentration, showing that the

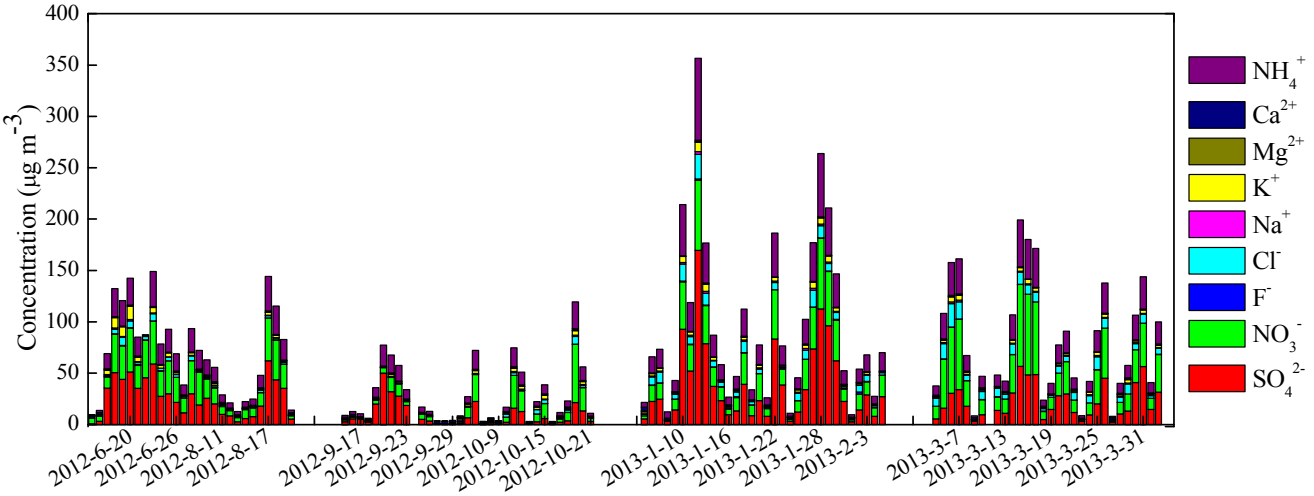

Fig. 3. Variations of the daily mass concentration of nine WSIIs in $PM_{2.5}$.

Table 1. Average concentrations of $PM_{2.5}$, chemical species (μg m^{-3}) and meteorological parameters.

Species	Annual	Summer	Autumn	Winter	Spring
$PM_{2.5}$	112.4 ± 94.4	103.3 ± 62.2	58.3 ± 49.2	169.1 ± 130.4	119.6 ± 76.1
SO_4^{2-}	24.2 ± 26.1	26.3 ± 18.3	9.38 ± 11.5	38.9 ± 38.9	22.8 ± 16.7
NO_3^-	20.3 ± 19.1	21.6 ± 13.5	9.12 ± 12.5	22.7 ± 18.6	29.5 ± 24.0
F^-	0.22 ± 0.33	0.28 ± 0.30	0.07 ± 0.08	0.42 ± 0.50	0.10 ± 0.14
Cl^-	4.33 ± 0.61	2.37 ± 2.08	0.99 ± 1.61	6.45 ± 5.33	7.62 ± 5.02
Na^+	0.61 ± 0.51	0.46 ± 0.35	0.30 ± 0.43	0.92 ± 0.60	0.77 ± 0.36
K^+	2.20 ± 2.18	2.71 ± 3.29	1.31 ± 1.12	2.70 ± 2.26	2.20 ± 1.30
Mg^{2+}	0.16 ± 0.11	0.16 ± 0.07	0.19 ± 0.08	0.16 ± 0.17	0.10 ± 0.07
Ca^{2+}	1.11 ± 0.56	0.90 ± 0.34	1.15 ± 0.51	0.78 ± 0.54	1.61 ± 0.47
NH_4^+	15.8 ± 13.7	16.2 ± 9.9	6.91 ± 7.18	22.4 ± 11.3	18.4 ± 11.9
OC	17.1 ± 17.1	9.28 ± 5.85	8.62 ± 6.93	33.2 ± 23.4	16.1 ± 10.2
EC	5.60 ± 5.13	3.57 ± 2.00	3.59 ± 3.06	9.16 ± 6.94	5.80 ± 4.58
TEMP/°C	11.2 ± 11.1	25.3 ± 2.07	17.5 ± 3.70	–3.68 ± 1.81	6.91 ± 2.65
RH/%	58.8 ± 17.6	71.4 ± 15.1	53.4 ± 14.4	65.0 ± 17.4	47.8 ± 14.6
WS/m s^{-1}	2.09 ± 0.81	2.09 ± 0.45	1.91 ± 0.89	1.84 ± 0.76	2.57 ± 0.86
PR/mm	1.31 ± 4.98	4.79 ± 9.64	0.71 ± 2.41	0.19 ± 0.58	0.35 ± 1.29

percentages of WSIIs in $PM_{2.5}$ was higher than those measured in 2009 (Zhang *et al.*, 2013). Secondary inorganic aerosols (SNA, including SO_4^{2-}, NO_3^- and NH_4^+) were major components of WSIIs, comprising 80.3% of annual average total WSIIs. From a seasonal perspective, SO_4^{2-} had the highest concentration in winter and the lowest concentration in autumn. The higher concentrations of SO_4^{2-} in winter might be caused by the coal combustion for residential heating.

The seasonal variations of NO_3^- were different from SO_4^{2-}. Vehicular exhaust was the main source of NO_x, while coal combustion may also contribute to NO_x (Zhang, 2014). The maximum concentrations of NO_3^- were observed in spring. The coal burning for residential heating in early spring may release NO_x, resulting in relatively higher NO_3^- concentration. Although high temperature may promote photochemical processes, NO_3^- was observed slightly lower in summer than spring due to the evaporation from filter at high temperature. Meanwhile, the variation of NH_4^+ was consistent with that of $PM_{2.5}$. The lowest concentration of NH_4^+ was observed in summer, which may also be caused by evaporating from the filters at high temperature.

First, we assumed that the presence of NH_4^+ and SO_4^{2-} was in the form of $(NH_4)_2SO_4$ rather than NH_4HSO_4. The charge balance between $[NH_4^+]$ and $[SO_4^{2-}+NO_3^-]$ was analyzed in the present study (Fig. 4). The slope of the linear regression was 0.990 with a correlation coefficient R^2 = 0.985, indicating that the SO_4^{2-} and NO_3^- were fully neutralized by NH_3 in the form of $(NH_4)_2SO_4$ and NH_4NO_3. According to the charge balance, the calculated concentrations of NH_4^+ were well correlated to the measured one, with a relationship of y = 0.986x and a correlation coefficient R^2 = 0.982. Thus, $(NH_4)_2SO_4$ and NH_4NO_3 can be estimated by the SO_4^{2-} and NO_3^- mass concentration multiplied by a factor of 1.38 and 1.29, respectively.

Previous study has shown that Cl^- might be derived from coal combustion when the Cl^-/Na^+ equivalent concentration ratios were larger than the mean ratio (1.17) for sea water (Wang *et al.*, 2006). The ratios of $[Cl^-]/[Na^+]$ were 3.35, 2.14, 4.55, and 6.41 in summer, autumn, winter, and spring,

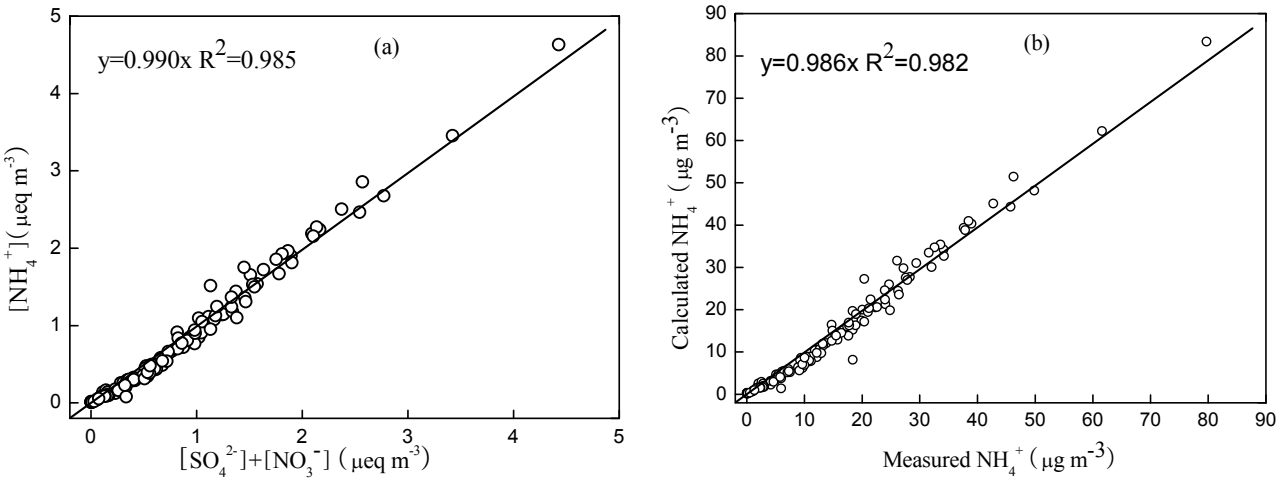

Fig. 4. Linear relationships of $[NH_4^+]$ versus $[NO_3^- + SO_4^{2-}]$ (a) and correlation between calculated and measured concentration of NH_4^+ (b).

respectively, indicating that the higher concentrations of Cl^-, especially in winter, were caused by the increased amount of coal combustion for heating. Ca^{2+} would be more likely originated from the re-suspended road dust and long-range transported dust (Gao *et al*., 2014). Concentrations of Ca^{2+} were highest in the spring, which might be ascribed to the high loading of crustal dust due to strong wind in spring. K^+ had a higher concentration in both summer and winter than in spring and autumn. Wheat straw burning during the summer harvest may cause the elevated concentration of K^+, while the high concentrations of K^+ in winter may be related to the biomass burning for residential heating.

Annual Average and Seasonal Variations of Carbonaceous Compounds

Carbonaceous aerosols accounted for 20.6%, 31.8%, 39.4%, and 23.9% of $PM_{2.5}$ in summer, autumn, winter, and spring, respectively, with an annual average of 29.6%. Temporal variations of OC, EC and OC/EC in $PM_{2.5}$ are shown in Fig. 5, and summary statistics of OC and EC among four seasons are listed in Table 1. The annual average mass concentration of OC and EC in $PM_{2.5}$ was 17.1 ± 17.1 μg m^{-3} and 5.6 ± 5.1 μg m^{-3}, respectively, which were lower than those observed in previous years (Duan *et al*., 2006; Wang *et al*., 2011; Yang *et al*., 2011b; Zhou *et al*., 2012), but close to those observed most recently (Zhang *et al*., 2013; Zhao *et al*., 2013c). These lower OC and EC levels were mainly due to energy restructuring. Beijing has largely switched from residential and industrial coal to natural gas or central steam since 2006.

The seasonal variations of OC and EC showed similar patterns to that of $PM_{2.5}$ mass, with higher concentrations in winter and spring, and lower concentrations in summer and autumn. The higher concentrations in winter and spring can be explained by a combination of emission source and meteorological conditions. There was a ''heating season'' from November to the following March in Beijing. Coal combustion and biomass burning for local heating were likely a cause of high OC and EC levels. On the other hand, low wind speed and low precipitation during winter were conductive to the accumulation of pollutants, contributing to the high carbon loading.

OC concentrations were all higher than those of EC during all sampling periods. The SOC concentrations could be estimated roughly using the minimum OC/EC ratio method, which suggested that samples having the lowest OC/EC ratio contained almost exclusively primary organic aerosols (POC) (Castro *et al*., 1999). Then, the concentrations of SOC can be estimated by the following equations:

$$POC = EC \times (OC/EC)_{min} \quad (4)$$

$$SOC = OC - POC \quad (5)$$

where $(OC/EC)_{min}$ was the value of the lowest OC/EC ratio. Since the validity of the $(OC/EC)_{min}$ was crucial to calculate the POC, three samples with the lowest OC/EC ratios were used during a given season (Lim and Turpin, 2002; Yuan *et al*., 2006). Based on the $(OC/EC)_{min}$ of 1.63, 1.46, 2.17 and 2.26 in summer, autumn, winter and spring, the average concentrations of SOC were 3.53, 3.53, 13.4, and 2.99 μg m^{-3}, which accounted for 35.3%, 40.7%, 42.6%, and 13.1% of OC, respectively. Similar to SNA, SOC were highest in winter. The stable atmosphere and cool temperature in winter could facilitate accumulation of air pollutants and accelerate the condensation of volatile organic compounds onto particles. The concentrations of SNA were higher in spring, and the lowest in autumn. While the concentrations of SOC were equal in summer and autumn, and the lowest concentration appeared in spring. In the spring, the wind was strong, and the pollutants have been dispersed, which was unfavorable for the OC aging and thereby caused lower SOC formation. Thus, the higher concentrations of OC in spring might almost be fresh particles.

Chemical Mass Balance

As shown in Fig. 6, the reconstructed $PM_{2.5}$ mass was significantly correlated with the measured value ($R^2 > 0.98$) during the four seasons. This implied that the reconstruction of eight major components in $PM_{2.5}$ adopted in this study

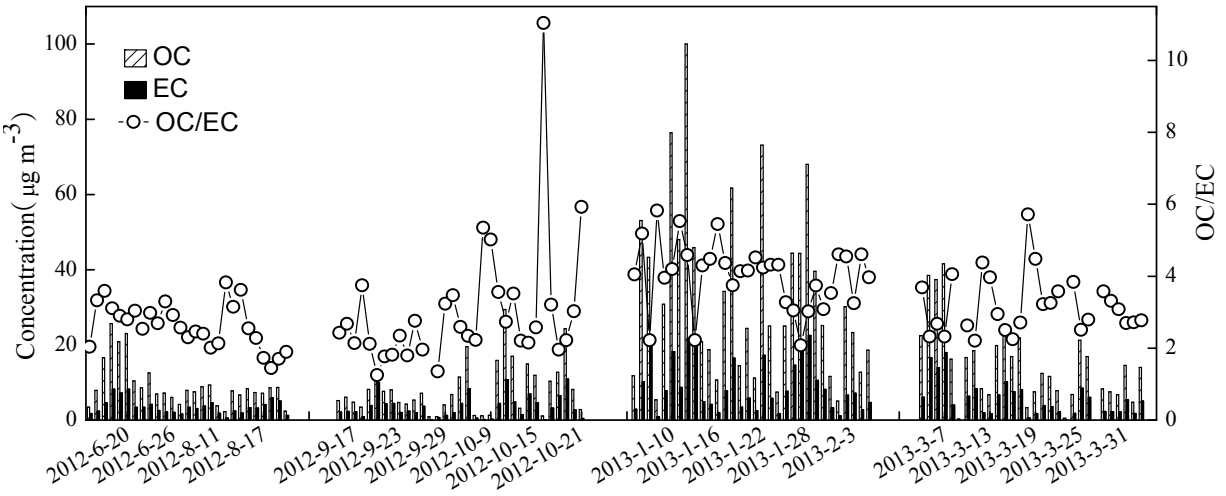

Fig. 5. Temporal variations of OC, EC and OC/EC in $PM_{2.5}$.

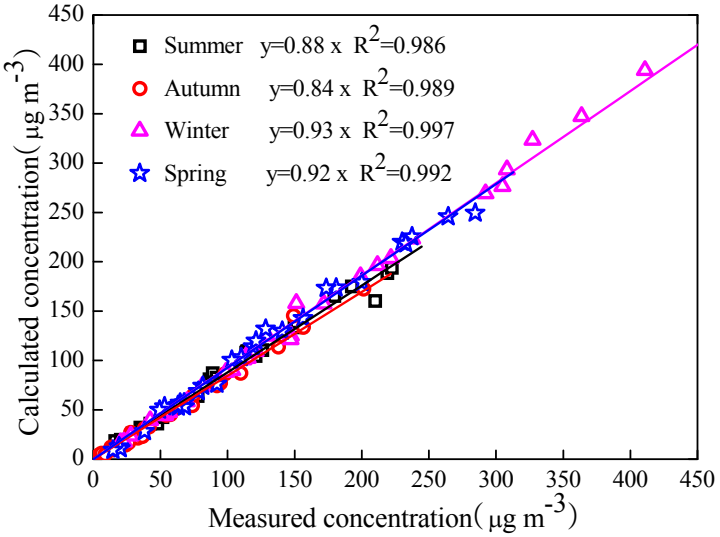

Fig. 6. Scatter plots of measured and calculated $PM_{2.5}$ mass concentrations by season.

was reasonable. Compared with measured $PM_{2.5}$ mass, the reconstructed values were found to be underestimated by 13% on average, but about 20% in autumn. The underestimation of the reconstructed $PM_{2.5}$ mass was mainly associated with two factors. The water-soluble components such as NO_3^-, SO_4^{2-} and NH_4^+ are likely to be absorbed by water during weighting, which may lead to positive biases in measured $PM_{2.5}$ mass concentration (Tsai and Kuo, 2005). Additionally, the factor used in converting a given analyzed species to a certain component was critical for $PM_{2.5}$ mass reconstruction. The factor of 1.8 has been used for the conversion of OM from OC in previous studies (Yang *et al.*, 2012; Tao *et al.*, 2013), which was related to the quantities of aging organic matter. If we adopted the factor of 1.8 to estimate the OM mass in autumn and winter, the underestimation will be reduced by 3%.

Contributions of Each Chemical Component to Light Extinction

The seasonal variations of b_{ext} as well as the contribution of each species to b_{ext} are shown in Fig. 7. The value of b_{ext} was highest in winter (1427.4 ± 1274.3 Mm^{-1}), followed by summer and spring (877.3 ± 586.5 and 841.3 ± 589.3 Mm^{-1}, respectively), and lowest in autumn (384.9 ± 381.7 Mm^{-1}), with an annual b_{ext} value of 879.9 ± 872.7 Mm^{-1}. Compared with other cities in China, the annual value of b_{ext} observed in Beijing was much higher than that observed in Xiamen and Guangzhou (Zhang *et al.*, 2012; Tao *et al.*, 2014), comparable with that observed in Jinan and Chengdu (Yang *et al.*, 2012; Song *et al.*, 2013), but was lower than that obtained in Xi'an (Cao *et al.*, 2012). Compared with other b_{ext} values obtained in Beijing, the value of b_{ext} in this study was higher than that observed in 2008 (Li *et al.*, 2013a) and 2012 (Tian *et al.*, 2014), and comparable with that obtained in 2006 (Jung *et al.*, 2009). The highest b_{ext} in winter may be associated with the high concentrations of $PM_{2.5}$. Furthermore, $PM_{2.5}$ mass concentration was found to be higher in spring than summer, while the b_{ext} value had a distinctly contrasting pattern with slightly higher values in summer than spring. The phenomenon may be due to the

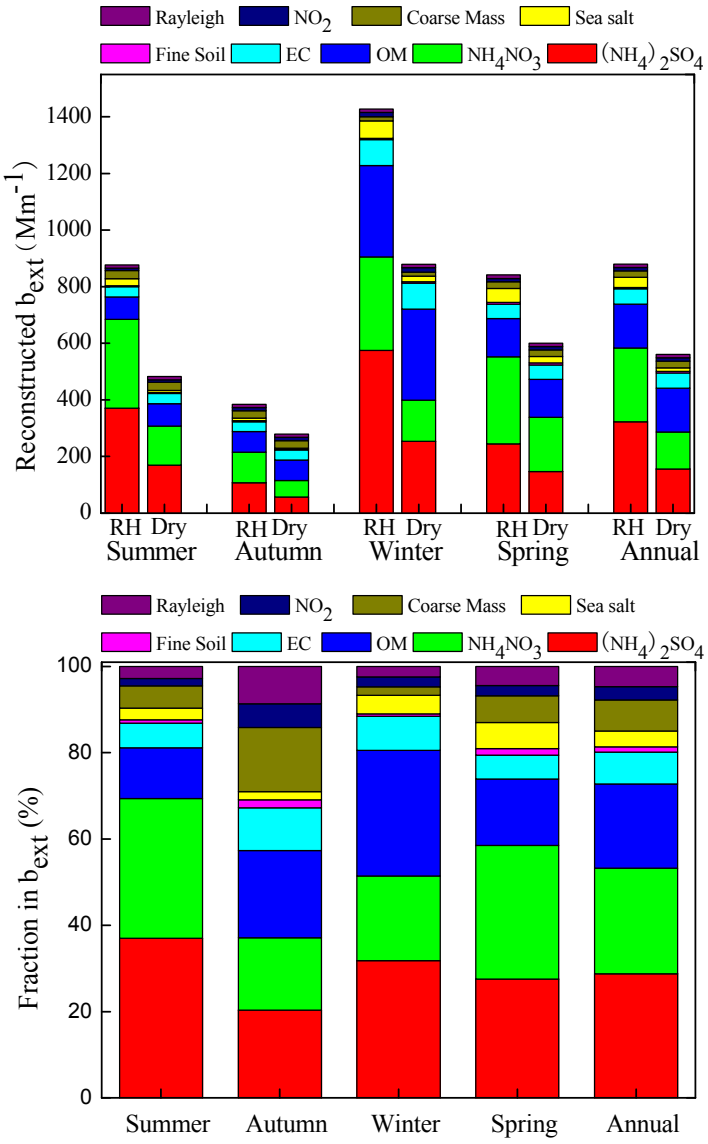

Fig. 7. Seasonal variations of b_{ext} and relative contributions of each species to the total b_{ext}.

high relative humidity in summer. Previous studies showed that hygroscopic species such as $(NH_4)_2SO_4$ and NH_4NO_3 can absorb water vapor, which can significantly influence its particle size as relative humidity increased, thus enhancing the scattering coefficient and proportionately reducing visibility (Malm and Day, 2001; Malm *et al.*, 2003).

Dry extinction coefficients ($b_{ext,dry}$) were estimated by Eq. (3) with f(RH) = 1, while ambient extinction coefficients (b_{ext}) were estimated using Eq. (3) in which the hygroscopic growth of inorganic components was considered. As illustrated in Fig. 7, average reconstructed $b_{ext,dry}$ was 560.3 ± 492.2 Mm^{-1}, while b_{ext} dependent on the magnitude of RH, reached to 879.9 ± 872.7 Mm^{-1}. The difference between average $b_{ext,dry}$ and b_{ext} was 26.6% during the entire four seasons. It is worth noting that the difference between $b_{ext,dry}$ and b_{ext} was as high as 37.9% in summer, whereas it was only 23.6% in spring. As discussed above, it was mainly attributed to SNA water absorption at higher relative humidity that the b_{ext} was larger in summer than spring despite higher concentrations being observed in spring rather than summer.

As shown in Fig. 7, during the entire study period, $(NH_4)_2SO_4$, NH_4NO_3 and OM, the three dominant chemical species, accounted for 72.7% of the total b_{ext}. $(NH_4)_2SO_4$ was the largest contributor to b_{ext}, accounting for 28.8%, followed by NH_4NO_3 (24.4%), OM (19.5%), EC (7.39%), and coarse mass (7.23%), while fine soil, sea salt, NO_2 and Rayleigh made a minor contribution, together accounting for 12.7%. It should be noted that there was an evident seasonal variations in contributions to b_{ext} from each species. The sum contributions of $(NH_4)_2SO_4$ and NH_4NO_3 to b_{ext} were the largest in summer, accounting for 69.4% of b_{ext}, while it decreased to 37.1% in autumn. It implied that gas-particle conversion was a likely key path for the accumulation of fine particles in summer. Another reason for the higher percentage of $(NH_4)_2SO_4$ and NH_4NO_3 in summer was their ability to absorb water vapor, which can enhance b_{ext} under high relative humidity. In contrast, the contribution of OM was the lowest in summer, accounting only for 11.7%, while it

approximated 2.5 times higher in winter than that in summer, which is closely related to the relatively high concentrations of OM in winter. Furthermore, the contributions of coarse mass, EC, and Rayleigh to b_{ext} could not be ignored during autumn.

The air quality index (AQI) is an index for reporting daily air quality (http://www.airnow.gov/index.cfm?action =aqibasics.aqi). In Beijing, $PM_{2.5}$ was the primary pollutant, thus, the AQI in this study was calculated according to the concentration of $PM_{2.5}$. In addition, the value of AQI was published on line every day by Beijing Municipal Environmental Protection Bureau, thus, it is interesting to discuss the extinction under different AQI. The air quality conditions were classified into six categories from the best to the worse according to AQI: stage I (AQI ≤ 50), stage II (51 ≤ AQI ≤ 100), stage III (101 ≤ AQI ≤ 150), stage IV (151 ≤ AQI ≤ 200), stage V (201 ≤ AQI ≤ 300), and stage VI (AQI > 300). Since the chemical components did not change significantly during the polluted periods, only stage I (clean period) and VI (polluted period) were compared during the entire sampling periods in Fig. 8. The fractions of the extinction coefficients caused by particles increased from 81.2% during stage I to 98.9% in stage VI. The dominant contributors to b_{ext} were coarse mass, Rayleigh, OM and $(NH_4)_2SO_4$ under stage I, accounting for 21.2%, 15.9%, 18.3%, and 14.2%, respectively. In contrast, it is noted that $(NH_4)_2SO_4$ and NH_4NO_3 were the main contributor to b_{ext} during stage VI, accounting for nearly 67.1%, but fine soil, coarse mass, NO_2 and Rayleigh had a minor contribution, together accounting for less than 3% of b_{ext}. It is apparent that the contribution of $(NH_4)_2SO_4$ and NH_4NO_3 to b_{ext} was much higher during the polluted air conditions than the clean air conditions, implying that $(NH_4)_2SO_4$ and NH_4NO_3 played a crucial role in the atmospheric visibility impairment in Beijing. OM and EC was fairly constant during the study period accounting for 18.8% and 7.04%, respectively, while the contribution of NO_2 and Rayleigh decreased sharply form stage I to VI, from 7.71% and 15.9% to 0.76% and 0.43%, respectively. As discussed above, it is worth noting that $(NH_4)_2SO_4$, NH_4NO_3 and OM were responsible for the reduced visibility in Beijing, thus, the reduction of their precursors like SO_2, NO_x and VOCs could effectively improve visibility in Beijing.

CONCLUSIONS

During the entire study, daily $PM_{2.5}$ mass concentrations ranged from 4.3 to 592.4 μg m^{-3} with an annual average of 112.4 ± 94.4 μg m^{-3}. The seasonal mass concentrations of $PM_{2.5}$ ranked in order of winter > spring > summer > autumn. WSIIs and carbonaceous compounds were the major contributors to $PM_{2.5}$ mass, accounting for 45.9% and 28.9% of the total, respectively. Overall, SO_4^{2-}, NO_3^- and NH_4^+ were major components of WSIIs, which comprised 80.7% of total WSIIs. The annual average mass concentrations of OC and EC in $PM_{2.5}$ were 17.1 ± 17.1 μg m^{-3} and 5.60 ± 5.13 μg m^{-3}, respectively. The seasonal variations of OC and EC had a similar trend to $PM_{2.5}$ mass. The OC/EC ratios varied from 2.64 to 4.02 with an annual average of 3.14, suggesting SOC might be present in Beijing.

Light extinction was reconstructed based on the chemical species using the revised IMPROVE formula over different seasons. The highest b_{ext} occurred in winter, followed by summer and spring, and the lowest in autumn, with an annual average value of 879.9 ± 872.7 Mm^{-1}. $(NH_4)_2SO_4$, NH_4NO_3 and OM were the three dominant chemical species, together accounting for 72.7% of the total b_{ext}. On average, $(NH_4)_2SO_4$ was the largest contributor of b_{ext}, accounting for 28.8%, followed by NH_4NO_3 (24.4%), OM (19.5%), EC (7.39%), and coarse mass (7.23%). Fine soil, sea salt, NO_2 and Rayleigh had a minor contribution, together accounting for 12.7%. The chemical species experienced different variations in their concentrations and contributions to the total b_{ext} under different pollution conditions. During the clean periods (stage I), the contributions of coarse mass and Rayleigh to b_{ext} were as high as 21.2% and 15.9%, respectively, while $(NH_4)_2SO_4$ and NH_4NO_3 contributed only

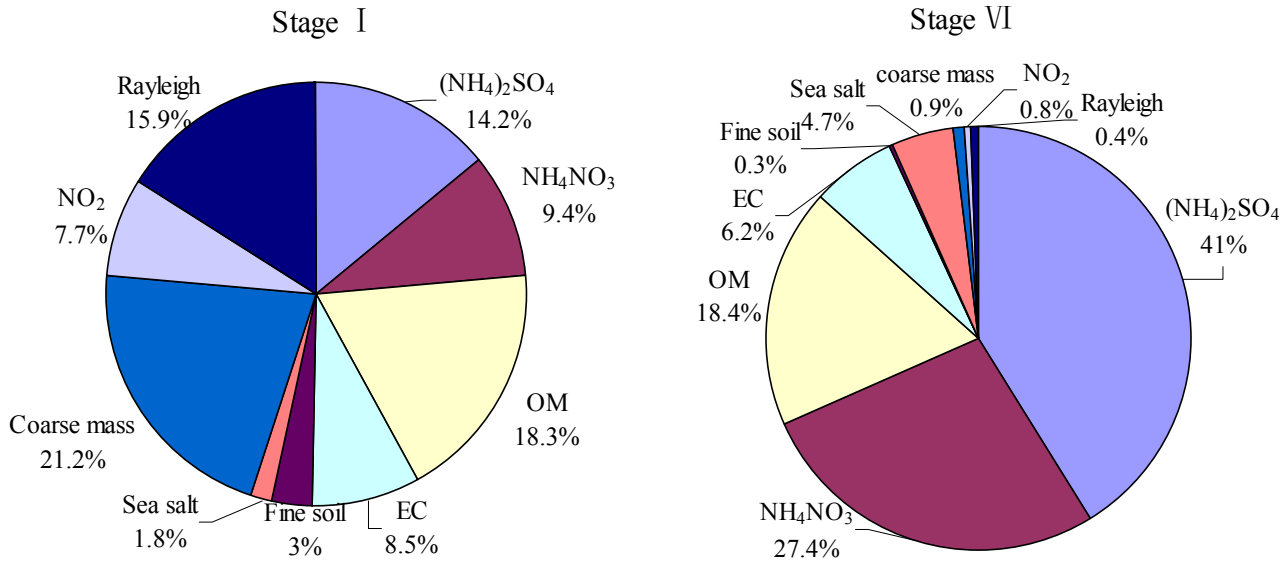

Fig. 8. Relative contributions of each species to b_{ext} under different AQI stages.

14.1% and 9.42%. During the polluted periods, $(NH_4)_2SO_4$ and NH_4NO_3 together accounted for 67.1% of b_{ext}, while coarse mass and Rayleigh had a minor contribution with a share of only 3.1%. Therefore, in addition to control primary particulate emissions, the reduction of secondary inorganic aerosols in $PM_{2.5}$ could be more effective in improving both air quality and visibility.

ACKNOWLEDGEMENTS

This work was supported by the National Natural Science Foundation of China projects (41075093, 41275121 and 41375123), the "Strategic Priority Research Program" of the Chinese Academy of Sciences (KJZD-EW -TZ-G06-04), Major Program for the Fundamental Research of the Ministry of Science and Technology of China (2013FY112700), the State Environmental Protection Key Laboratory of Sources and Control of Air Pollution Complex (SCAPC201310), the Ministry of Environmental Protection of China (201209007), Jiangsu Key Laboratory of Atmospheric Environment Monitoring and Pollution Control of Nanjing University of Information Science and Technology, and Jiangsu Province Innovation Platform for Superiority Subject of Environmental Science and Engineering (KHK1201). The authors thank Lianfang Wei, Qingqing Wang, Jinlu Dong, and Dr. Rong Zhang for their contributions to the field and laboratory work.

REFERENCES

Cao, J.J., Wang, Q.Y., Chow, J.C., Watson, J.G., Tie, X.X., Shen, Z.X., Wang, P. and An, Z.S. (2012). Impacts of Aerosol Compositions on Visibility Impairment in Xi'an, China. *Atmos. Environ.* 59: 559–566.

Castro, L.M., Pio, C.A., Harrison, R.M. and Smith, D.J.T. (1999). Carbonaceous Aerosol in Urban and Rural European Atmospheres: Estimation of Secondary Organic Carbon Concentrations. *Atmos. Environ.* 33: 2771–2781.

Chan, Y.C., Simpson, R.W., Mctainsh, G.H., Vowles, P.D., Cohen, D.D. and Bailey, G.M. (1999). Source Apportionment of Visibility Degradation Problems in Brisbane (Australia) Using the Multiple Linear Regression Techniques. *Atmos. Environ.* 33: 3237–3250.

Chang, D., Song, Y. and Liu, B. (2009). Visibility Trends in Six Megacities in China 1973–2007. *Atmos. Res.* 94: 161–167.

Chow, J.C., Watson, J.G., Chen, L.W.A., Chang, M.C.O., Robinson, N.F., Trimble D. and Kohl, S. (2007). The IMPROVE-A Temperature Protocol for Thermal/Optical Carbon Analysis: Maintaining Consistency with a Long-Term Database. *J. Air Waste Manage.* 57: 1014–1023.

De Kok, T.M.C.M., Driece, H.A.L., Hogervorst, J.G.F. and Briede, J.J. (2006). Toxicological Assessment of Ambient and Traffic-Related Particulate Matter: A Review of Recent Studies. *Mutat. Res. Rev. Mutat. Res.* 613: 103–122.

Duan, F.K., He, K.B., Ma, Y.L., Yang, F.M., Yu, X.C., Cadle, S.H., Chan, T. and Mulawa, P.A. (2006). Concentration and Chemical Characteristics of $PM_{2.5}$ in Beijing, China: 2001–2002. *Sci. Total Environ.* 355: 264–275.

Fan, X.H., Chen, H.B., Xia, X.G., Li, Z.Q. and Cribb, M. (2010). Aerosol Optical Properties from the Atmospheric Radiation Measurement Mobile Facility at Shouxian, China. *J. Geophys. Res.* 115: D00K06.

Garland, R.M., Schmid, O., Nowak, A., Achtert, P., Wiedensohler, A., Gunthe, S.S., Takegawa, N., Kita, K., Kondo, Y., Hu, M., Shao, M., Zeng, L.M., Zhu, T., Andreae, M.O. and Poschl, U. (2009). Aerosol Optical Properties Observed during Campaign of Air Quality Research in Beijing 2006 (CAREBeijing-2006): Characteristic Differences between the Inflow and Outflow of Beijing City Air. *J. Geophys. Res.* 114: D00G04,.

Gao, J.J., Tian, H.Z., Chen, K., Wang, Y.X., Wu., Y. and Zhu, C.Y. (2014). Seasonal and spatial variation of trace Elements in Multi-Size Airborne particulate Matters of Beijing, China: Mass Concentration, Enrichment Characteristics, Source Apportionment, Chemical Speciation and Bioavailability. *Atmos. Environ.* 99: 257–265.

Haywood, J. and Boucher, O. (2000). Estimates of the Direct and Indirect Radiative Forcing Due to Tropospheric Aerosols: A Review. *Rev. Geophys.* 38: 513–543.

He, K.B., Yang, F.M., Ma, Y.L., Zhang, Q., Yao, X.H., Chan, C.K., Cadle, S., Chan, T. and Mulawa, P. (2001). The Characteristics of $PM_{2.5}$ in Beijing, China. *Atmos. Environ.* 35: 4959–4970.

Ji, D.S., Li, L., Wang, Y.S., Zhang, J.K., Cheng, M.T., Sun, Y., Liu, Z.R., Wang, L.L., Tang, G.Q., Hu, B., Chao, N., Wen, T.X. and Miao, H.Y. (2014). The Heaviest Particulate Air-Pollution Episodes Occurred in Northern China in January, 2013: Insights Gained from Observation. *Atmos. Environ.* 92: 546–556.

Jung, J., Lee, H., Kim, Y.J., Liu, X.G., Zhang, Y.H., Hu, M. and Sugimoto, N. (2009). Optical Properties of Atmospheric Aerosols Obtained by in Situ and Remote Measurements during 2006 Campaign of Air Quality Research in Beijing (CAREBeijing-2006). *J. Geophys. Res.* 114: D00G02.

Li, X.H., He, K.B., Li, C.C., Yang, F.M., Zhao, Q., Ma, Y.L., Cheng, Y., Ouyang, W.J. and Chen, G.C. (2013a). $PM_{2.5}$ Mass, Chemical Composition, and Light Extinction Before and during the 2008 Beijing Olympics. *J. Geophys. Res.* 118: 12158–12167.

Li, X.R., Wang, L.L., Wang, Y.S., Wen, T.X., Yang, Y.J., Zhao, Y.N. and Wang, Y.F. (2012). Chemical Composition and Size Distribution of Airborne Particulate Matters in Beijing during the 2008 Olympics. *Atmos. Environ.* 50: 278–286.

Li, X.R., Wang, L.L., Ji, D.S., Wen, T.X., Pan, Y.P., Sun, Y. and Wang, Y.S. (2013b). Characterization of the Size-Segregated Water-Soluble Inorganic Ions in the Jing-Jin-Ji Urban Agglomeration: Spatial/Temporal Variability, Size Distribution and Sources. *Atmos. Environ.* 77: 250–259.

Lim, H.J. and Turpin, B.J. (2002). Origins of Primary and Secondary Organic Aerosol in Atlanta: Results' of Time-Resolved Measurements during the Atlanta Supersite Experiment. *Environ. Sci. Technol.* 36: 4489–4496.

Liu, Y.J., Zhang, T.T., Liu, Q.Y., Zhang, R.J., Sun, Z.Q. and Zhang, M.G. (2014). Seasonal Variation of Physical and

Chemical Properties in TSP, PM_{10} and $PM_{2.5}$ at a Roadside Site in Beijing and Their Influence on Atmospheric Visibility. *Aerosol Air Qual. Res.* 14: 954–969.

Mahowald, N. (2011). Aerosol Indirect Effect on Biogeochemical Cycles and Climate. *Science* 334: 794–796.

Malm, W.C. and Day, D.E. (2001). Estimates of Aerosol Species Scattering Characteristics as a Function of Relative Humidity. *Atmos. Environ*. 35: 2845–2860.

Malm, W.C., Day, D.E., Kreidenweis, S.M., Collett, J.L. and Lee, T. (2003). Humidity-Dependent Optical Properties of Fine Particles during the Big Bend Regional Aerosol and Visibility Observational Study. *J. Geophys. Res.* 108: D94279.

Pitchford, M., Malm, W., Schichtel, B., Kumar, N., Lowenthal, D. and Hand, J. (2007). Revised Algorithm for Estimating Light Extinction from Improve Particle Speciation Data. *J. Air Waste Manage.* 57: 1326–1336.

Pope, C.A. and Dockery, D.W. (2006). Health Effects of Fine Particulate Air Pollution: Lines That Connect. *J. Air Waste Manage.* 56: 709–742.

Quan, J.N., Tie, X.X., Zhang, Q., Liu, Q., Li, X., Gao, Y. and Zhao, D.L. (2014). Characteristics of Heavy Aerosol Pollution during the 2012–2013 Winter in Beijing, China. *Atmos. Environ.* 88: 83–89.

Song, D.L., Tao, J. and Zhang, P. (2013). Seasonal Characterization of Particle Extinction Coefficient and its Relation with $PM_{2.5}$ Mass Concentration in Chengdu. *J. Univ. Chin. Acad. Sci.* 30: 757–762.

Sun, K., Qu, Y., Wu, Q., Han, T.T., Gu, J.W., Zhao, J.J., Sun, Y.L., Jiang, Q., Gao, Z.Q., Hu, M., Zhang, Y.H., Lu, K.D., Nordmann, S., Cheng, Y.F., Hou, L., Ge, H., Furuuchi, M., Hata, M. and Liu, X.G. (2014). Chemical Characteristics of Size-Resolved Aerosols in Winter in Beijing. *J. Environ. Sci (China)* 26: 1641–1650.

Tai, A.P.K., Mickley, L.J. and Jacob, D.J. (2010). Correlations between fine particulate matter ($PM_{2.5}$) and Meteorological Variables in the United States: Implications for the Sensitivity of $PM_{2.5}$ to Climate Change. *Atmos. Environ.* 44: 3976–3984.

Tan, J.H., Duan, J.C., Chen, D.H., Wang, X.H., Guo, S.J., Bi, X.H., Sheng, G.Y., He, K.B. and Fu, J.M. (2009). Chemical Characteristics of Haze during Summer and Winter in Guangzhou. *Atmos. Res.* 94: 238–245.

Tao, J., Cheng, T.T., Zhang, R.J., Cao, J.J., Zhu, L.H., Wang, Q.Y., Luo, L. and Zhang, L.M. (2013). Chemical Composition of $PM_{2.5}$ at an Urban site of Chengdu in Southwestern China. *Adv. Atmos. Sci.* 30: 1070–1084.

Tao, J., Zhang, L.M., Ho, K.F., Zhang, R.J., Lin, Z.J., Zhang, Z.S., Lin, M., Cao, J.J., Liu, S.X. and Wang, G.H. (2014). Impact of $PM_{2.5}$ Chemical Compositions on Aerosol Light Scattering in Guangzhou - The Largest Megacity in South China. *Atmos. Res.* 135: 48–58.

Tian, P., Wang, G.F. and Zhang, R.J. (2014). Impacts of Aerosol Chemical Compositions on Optical Properties in Urban Beijing, China. *Particuology* 18: 155–164, doi: 10.1016/j.partic.2014.03.014.

Tsai, Y.I. and Kuo, S.C. (2005). $PM_{2.5}$ Aerosol Water Content and Chemical Composition in a Metropolitan and a Coastal Area in Southern Taiwan. *Atmos. Environ.* 39: 4827–4839.

Wang, Q.Y., Cao, J.J., Shen, Z.X., Tao, J., Xiao, S., Luo, L., He, Q.Y. and Tang, X.Y. (2013a). Chemical Characteristics of $PM_{2.5}$ during Dust Storms and air Pollution Events in Chengdu, China. *Particuology* 11: 70–77.

Wang, Q., Chen, X., He, G.L., Lin, S.B., Liu, Z. and Xu, D.Q. (2013b). Study on Characteristics of Elements in $PM_{2.5}$ during Haze-Fog Weather in Winter in Urban Beijing. *Spectrosc. Spect. Anal.* 33: 1441–1445.

Wang, S.X., Xing, J., Chatani, S., Hao, J.M., Klimont, Z., Cofala, J. and Amann, M. (2011). Verification of Anthropogenic Emissions of China by Satellite and Ground Observations. *Atmos. Environ.* 45: 6347–6358.

Wang, X.H., Bi, X.H., Sheng, G.Y. and Fu, J.M. (2006). Chemical Composition and Sources of PM_{10} and $PM_{2.5}$ Aerosols in Guangzhou, China. *Environ. Monit. Assess.* 119: 425–439.

Wang, Y.S., Yao, L., Wang, L.L., Liu, Z.R., Ji, D.S., Tang, G.Q., Zhang, J.K., Sun, Y., Hu, B. and Xin, J.Y. (2014). Mechanism for the Formation of the January 2013 Heavy Haze Pollution Episode over Central and Eastern China. *Sci. China Earth Sci.* 57: 14–25.

Watson, J.G. (2002). Visibility: Science and Regulation. *J. Air Waste Manage.* 52: 628–713.

Xing, L., Fu, T.M., Cao, J.J., Lee, S.C., Wang, G.H., Ho, K.F., Cheng, M.C., You, C.F. and Wang, T.J. (2013). Seasonal and Spatial Variability of the OM/OC Mass Ratios and High Regional Correlation between Oxalic Acid and Zinc in Chinese Urban Organic Aerosols. *Atmos. Chem. Phys.* 13: 4307–4318.

Xu, H.M., Cao, J.J., Ho, K.F., Ding, H., Han, Y.M., Wang, G.H., Chow, J.C., Watson, J.G., Khol, S.D., Qiang, J. and Li, W.T. (2012a). Lead Concentrations in fine Particulate Matter after the Phasing Out of Leaded Gasoline in Xi'an, China. *Atmos. Environ*. 46: 217–224.

Xu, L.L., Chen, X.Q., Chen, J.S., Zhang, F.W., He, C., Zhao, J.P. and Yin, L.Q. (2012b). Seasonal Variations and Chemical Compositions of $PM_{2.5}$ Aerosol in the Urban Area of Fuzhou, China. *Atmos. Res.* 104: 264–272.

Yang, F., Tan, J., Zhao, Q., Du, Z., He, K., Ma, Y., Duan, F., Chen G. and Zhao, Q. (2011a). Characteristics of $PM_{2.5}$ Speciation in Representative Megacities and across China. *Atmos. Chem. Phys.* 11: 5207–5219.

Yang, F., Huang, L., Duan, F., Zhang, W., He, K., Ma, Y., Brook, J.R., Tan, J., Zhao, Q. and Cheng, Y. (2011b). Carbonaceous Species in $PM_{2.5}$ at a Pair of Rural/Urban Sites in Beijing, 2005–2008. *Atmos. Chem. Phys.* 11: 7893–7903.

Yang, L.X., Zhou, X.H., Wang, Z., Zhou, Y., Cheng, S.H., Xu, P.J., Gao, X.M., Nie, W., Wang, X.F. and Wang, W.X. (2012). Airborne Fine Particulate Pollution in Jinan, China: Concentrations, Chemical Compositions and Influence on Visibility Impairment. *Atmos. Environ.* 55: 506–514.

Yao, X.H., Chan, C.K., Fang, M., Cadle, S., Chan, T., Mulawa, P., He, K.B. and Ye, B.M. (2002). The Water-Soluble Ionic Composition of $PM_{2.5}$ in Shanghai and

Beijing, China. *Atmos. Environ.* 36: 4223–4234.

Yu, L.D., Wang, G.F., Zhang, R.J., Zhang, L.M., Song, Y., Wu, B.B., Li, X.F., An, K. and Chu, J.H. (2013). Characterization and Source Apportionment of $PM_{2.5}$ in an Urban Environment in Beijing. *Aerosol Air Qual. Res.* 13: 574–583.

Yuan, Z.B., Yu, J.Z., Lau, A.K.H., Louie, P.K.K. and Fung, J.C.H. (2006). Application of Positive Matrix Factorization in Estimating Aerosol Secondary Organic Carbon in Hong Kong and Its Relationship with Secondary Sulfate. *Atmos. Chem. Phys.* 6: 25–34.

Zhang, F.W., Xu, L.L., Chen, J.S., Yu, Y.K., Niu, Z.C. and Yin, L.Q. (2012). Chemical Compositions and Extinction Coefficients of $PM_{2.5}$ in Peri-Urban of Xiamen, China, during June 2009–May 2010. *Atmos. Res.* 106: 150–158.

Zhang, R., Jing, J., Tao, J., Hsu, S.C., Wang, G., Cao, J., Lee, C.S.L., Zhu, L., Chen, Z., Zhao, Y. and Shen, Z. (2013). Chemical Characterization and Source Apportionment of $PM_{2.5}$ in Beijing: Seasonal Perspective. *Atmos. Chem. Phys.* 13: 7053–7074.

Zhang, X.Y. (2014). Characteistics of the Chemical Components of Aerosol Particles in the Various Regions over China. *Acta Meteorol. Sin.* 72: 1108–1117.

Zhao, P.S., Zhang, X.L., Xu, X.F. and Zhao, X.J. (2011). Long-Term Visibility Trends and Characteristics in the Region of Beijing, Tianjin, and Hebei, China. *Atmos. Res.* 101: 711–718.

Zhao, X.J., Zhao, P.S., Xu, J., Meng, W., Pu, W.W., Dong, F., He, D. and Shi, Q.F. (2013a). Analysis of a Winter Regional Haze Event and Its Formation Mechanism in the North China Plain. *Atmos. Chem. Phys.* 13: 5685–5696.

Zhao, P.S., Dong, F., Yang, Y.D., He, D., Zhao, X.J., Zhang, W.Z., Yao, Q. and Liu, H.Y. (2013b). Characteristics of Carbonaceous Aerosol in the Region of Beijing, Tianjin, and Hebei, China. *Atmos. Environ.* 71: 389–398.

Zhao, P.S., Dong, F., He, D., Zhao, X.J., Zhang, X.L., Zhang, W.Z., Yao, Q. and Liu, H.Y. (2013c). Characteristics of Concentrations and Chemical Compositions for $PM_{2.5}$ in the Region of Beijing, Tianjin, and Hebei, China. *Atmos. Chem. Phys.* 13: 4631–4644.

Zhou, J.M., Zhang, R.J., Cao, J.J., Chow, J.C. and Watson, J.G. (2012). Carbonaceous and Ionic Components of Atmospheric Fine Particles in Beijing and Their Impact on Atmospheric Visibility. *Aerosol Air Qual. Res.* 12: 492–502.

Received for review, April 25, 2015
Revised, June 16, 2015
Accepted, June 29, 2015